

Mapping solar irradiation from ground- and satellite-based data over Thailand using a simple semi-empirical model

Wanchalerm Chanalert, Korntip Tohsing*, Serm Janjai and Yowvanan Panjainam

Department of Physics, Faculty of Science, Silpakorn University, Nakhon Pathom 73000, Thailand

ABSTRACT

***Corresponding author:**
Korntip Tohsing
tohsing_k@silpakorn.edu

Received: 12 November 2021
Revised: 25 January 2022
Accepted: 14 March 2022
Published: 26 October 2022

Citation:
Chanalert, W., Tohsing, K.,
Janjai, S., and Panjainam, Y.
(2022). Mapping solar
irradiation from ground- and
satellite-based data over
Thailand using a simple semi-
empirical model. *Science,
Engineering and Health
Studies*, 16, 22020002.

An approach for mapping solar irradiation from ground and satellite-based data for Thailand was developed. A simple semi-empirical model relating normalized monthly average global solar irradiation to a normalized monthly average of visibility, precipitable water, total ozone column, and cloud index was proposed. Visibility data collected at 80 Thai meteorological stations were employed to represent the influence of aerosols on solar irradiation. Precipitable water was derived from air temperature and relative humidity measured at these stations. An interpolation technique was used to fill out the gaps between stations. Ozone data were acquired from OMI/AURA satellite data. A cloud index, which is used to represent the influence of clouds on irradiation, was calculated from MTSAT-1R satellite data. The model was based on global irradiation measured at four solar radiation monitoring stations located in the main regions of Thailand. The model validation using independent data at 36 stations revealed that the monthly average global solar irradiation computed from the model and that obtained from the measurements were in good agreement, with the root mean square difference being 6.9%. After its validation, the model was used to create solar irradiation maps. These maps are similar to those obtained from sophisticated irradiation models.

Keywords: solar irradiation; satellite data; semi-empirical model; mapping

1. INTRODUCTION

The geographical distribution of global solar irradiation is essential for solar energy applications (Duffie and Beckmann, 2013). Specifically, solar irradiation is a source of solar energy systems. Solar irradiation is also important for atmospheric research (Salby, 1996) because solar radiation supplies energy to the atmospheric system. A classical approach to obtain such information on solar irradiation is to establish a dense network of pyranometers in an area of interest and continuously measure incident solar irradiation for several years. Then, the average irradiation obtained from the network is presented on a geographical map of the area, and the

contour lines of solar irradiation are traced on that map to show the geographical distribution of the solar irradiation of that area (Suwantragul et al., 1984). Although networks of pyranometers have been established in many areas of the world, the density of pyranometers in most areas, especially in developing countries, is still low (Department of Alternative Energy Development and Efficiency, 2007; Department of Alternative Energy Development and Efficiency, 2009). The use of the measurement approach is generally simple, but its performance depends strongly on the density of the pyranometer network. As meteorological satellites can detect clouds over large areas and clouds are a main factor affecting surface solar irradiation, a number of researchers

have proposed methods for deriving surface solar irradiation from the imagery data of meteorological satellites (Möser and Raschke, 1984; Pinker and Laszlo, 1992; Exell, 2007; Cano et al., 1986; Wyser et al., 2002; Polo et al., 2011; Polo, 2015; Huang et al., 2019). The satellite approach consists of several techniques. These techniques can be broadly categorized as techniques using physical models and techniques employing statistical or empirical models. The physical model has an advantage in terms of generality, but it is relatively complicated and requires input data, which are not always available. The empirical model is generally simple, but it usually lacks generality. For the case of Thailand, the mapping of surface solar irradiation has been performed using various techniques (Exell, 2007; Sorapipatana et al., 1988; Janjai et al., 2005; Janjai et al., 2013a). These techniques include those based on measurements and those that use physical models. Each technique has advantages and disadvantages, as mentioned above. In this work, we proposed to map solar irradiation with ground- and satellite-based data over Thailand by using a simple semi-empirical model.

2. MATERIALS AND METHODS

2.1 Materials

The materials used in this work were satellite and ground-based data. The details of these data are described as follows.

2.1.1 Satellite data

The satellite data used in this approach were hourly imagery visible data from the MTSAT-1R satellite encompassing the period of 1 January 2006–31 December 2015. For each day, the hourly satellite data from 8:30 to 16:30 local time were used. The data were processed using the same method as that in our previous work (Janjai et al., 2013b). The information in each satellite pixel is the earth-atmospheric reflectivity (ρ_{EA}). Then, this information is converted into a cloud index (n) using a relation given by Cano et al. (1986) as:

$$n = \frac{\rho_{EA} - \rho_G}{\rho_c - \rho_G} \quad (1)$$

where ρ_G and ρ_c are the surface reflectivity and maximum cloud reflectivity, respectively.

As ozone absorbs solar irradiation and the amount of ozone from ground-based measurements is rarely available, the information on the amount of ozone obtained from the OMI/AURA satellite for the period of 2006–2015 was also acquired for this work.

2.1.2 Ground-based data

Data on global solar irradiation are essential for the formulation of the proposed semi-empirical model. In this work, the global solar irradiation measured at the following solar monitoring stations was collected: Chiang Mai station (18.78° N, 98.98° E) located in the northern region of Thailand, Ubon Ratchathani station (15.25° N, 104.87° E) situated in the Thai northeastern region, Nakhon Pathom station (13.82° N, 100.04° E) located in the Thai central region, and Songkhla station (7.20° N, 100.60° E) situated in the southern region of the country

(Figure 1). The data from these stations, covering the 10-year period (2006–2015), were used to formulate the semi-empirical model. The global solar irradiation measured at 36 stations of the Department of Alternative Energy Development and Efficiency (DEDE) of Thailand for a period of 1–5 years was also collected to validate the model. The positions of these DEDE stations are shown in Figure 1.

Water vapor absorbs a considerable amount of solar radiation (Iqbal, 1983; Kämpfer, 2013). In this study, precipitable water (w) was used to quantify water vapor, and w was estimated from ambient air temperature (T_a) and ambient relative humidity (rh_a) using the following formula proposed by Janjai et al. (2005):

$$w = 0.8933 \exp(0.1715 \frac{rh_a p_s}{T_a}) \quad (2)$$

where w is the precipitable water (cm), T_a is the temperature of ambient air (K), rh_a is the relative humidity of ambient air (decimal), and p_s is the saturated water vapor (mbar). The data of T_a and rh_a measured at 80 meteorological stations were collected to estimate w . The gaps between stations were filled out using the interpolation approach (Press et al., 1992).

In this work, the influence of atmospheric aerosols was quantified using the visibility data measured at 80 stations in Thailand, and the interpolation approach (Press et al., 1992) was employed to fill out gaps in the measurement.

2.2 Modeling

Instead of developing a physical model or an empirical model, a semi-empirical model was proposed for calculating solar irradiation. In general, solar irradiation depends on cloud, water vapor, ozone, and aerosol (Iqbal, 1983). To investigate this dependence, this study plotted the normalized monthly average daily values of cloud index, precipitable water, total ozone column, and visibility from the four stations for the period of 2006–2015 against the normalized monthly average of daily solar irradiation.

Also, the following model was proposed:

$$\bar{H} = a_0 + a_1 \frac{\bar{VIS}}{\bar{VIS}_{max}} + a_2 \frac{\bar{W}}{\bar{W}_{max}} + a_3 \frac{\bar{O}_3}{\bar{O}_{3_{max}}} + a_4 \frac{\bar{n}}{\bar{n}_{max}} \quad (3)$$

where \bar{H} is the monthly average of daily global solar irradiation, \bar{H}_0 is the monthly average of daily extraterrestrial solar irradiation, \bar{VIS} is the monthly average of daily visibility, \bar{VIS}_{max} is the maximum monthly average of daily visibility, \bar{W} is the monthly average of daily precipitable water, \bar{W}_{max} is the maximum monthly average of daily precipitable water, \bar{O}_3 is the monthly average of daily total ozone column, $\bar{O}_{3_{max}}$ is the maximum monthly average of daily total ozone column, \bar{n} is the monthly average of daily cloud index, and \bar{n}_{max} is the maximum monthly average of daily cloud index. a_0 , a_1 , a_2 , a_3 , and a_4 are the empirical coefficients of the model.

The t -statistic can be used to demonstrate goodness of fit. A higher absolute value of a t -statistic with the same number of samples relates to a low probability that the relationship occurs by chance (Montgomery et al., 2012). R^2 , commonly called the coefficient of determination, is the proportion of variance in the dependence variable that can be explained by the independent variables (Dhakal, 2019).

Table 1 shows that the value of R^2 was relatively high and the absolute values of the t -statistic associated with a_1 , a_2 , a_3 , and a_4 were greater than 2 with very low p -value,

meaning that $\frac{\bar{n}}{n_{\max}}$, $\frac{\bar{W}}{W_{\max}}$, $\frac{\bar{O}_3}{O_{3\max}}$, and $\frac{\bar{VTS}}{VTS_{\max}}$ were statistically significant predictors of $\frac{\bar{H}}{H_0}$.

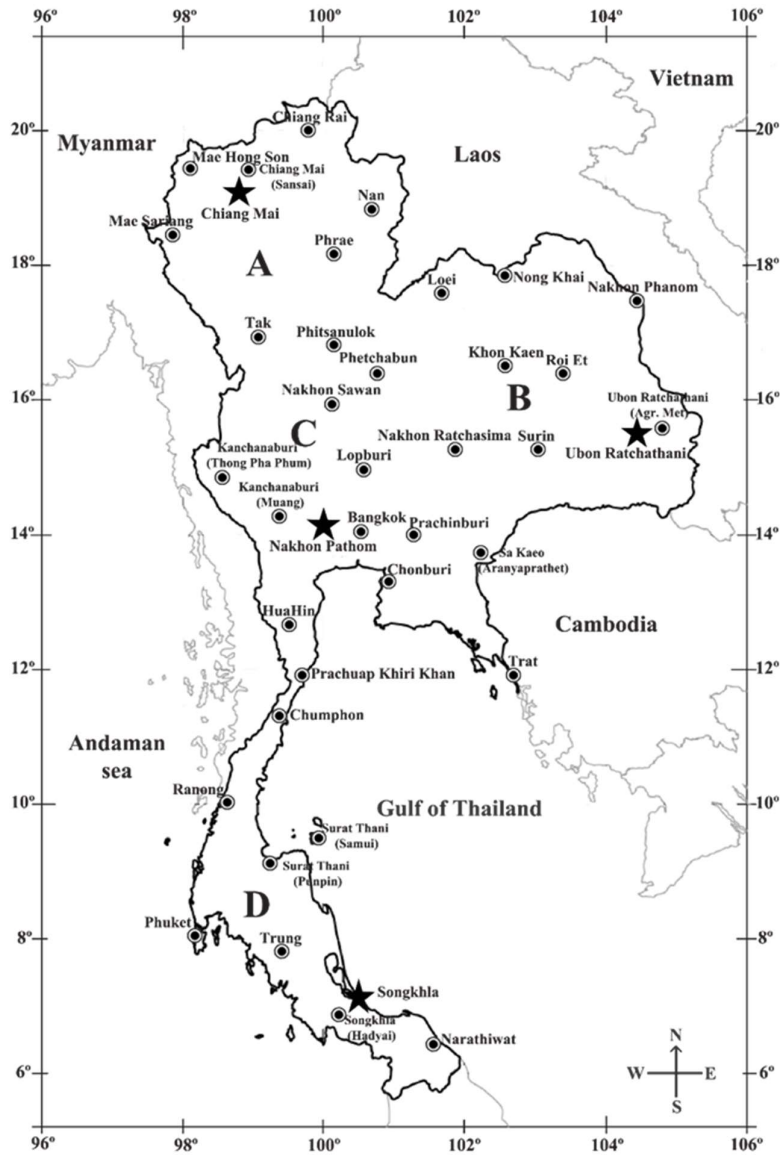


Figure 1. Map of Thailand showing the position of the solar monitoring stations (★) whose data were used to determine the model coefficients and the position of the DEDE stations (⊙)

Note: Data were employed for model validation (A, B, C, and D indicate the northern, northeastern, central, and southern regions, respectively).

Table 1. Values of model coefficients and statistical parameters

Coefficient	Value of coefficient	t -statistic	p -value	R^2	N
a_0	0.7425	20.8147	<0.05	0.79	480
a_1	0.0511	2.4155	<0.05		
a_2	0.0681	3.9264	<0.05		
a_3	-0.2241	-5.1937	<0.05		
a_4	-0.2545	-29.9436	<0.05		

Note: R is the correlation coefficient, and N is the total amount of data

3. RESULTS AND DISCUSSION

Figure 2 reveals the results. It indicates the degree of correlation between the variable on the vertical axis and horizontal axis. Ideally, correlation coefficient (R) should be 1 or -1. From Figure 2, the values of R in many cases were relatively low. Take for example the case of ozone: the parameters in the correlation between the dependent

variable $\frac{\bar{H}}{\bar{H}_0}$ and $\frac{\bar{O}_3}{\bar{O}_{3\max}}$, exerted certain influences, additionally, there were influences from other dependent variables in the graph, thus making the correlation coefficient low. In addition, we could not isolate these influences for the all-sky condition because the information on the solar spectrum under the all-sky conditions was not available.

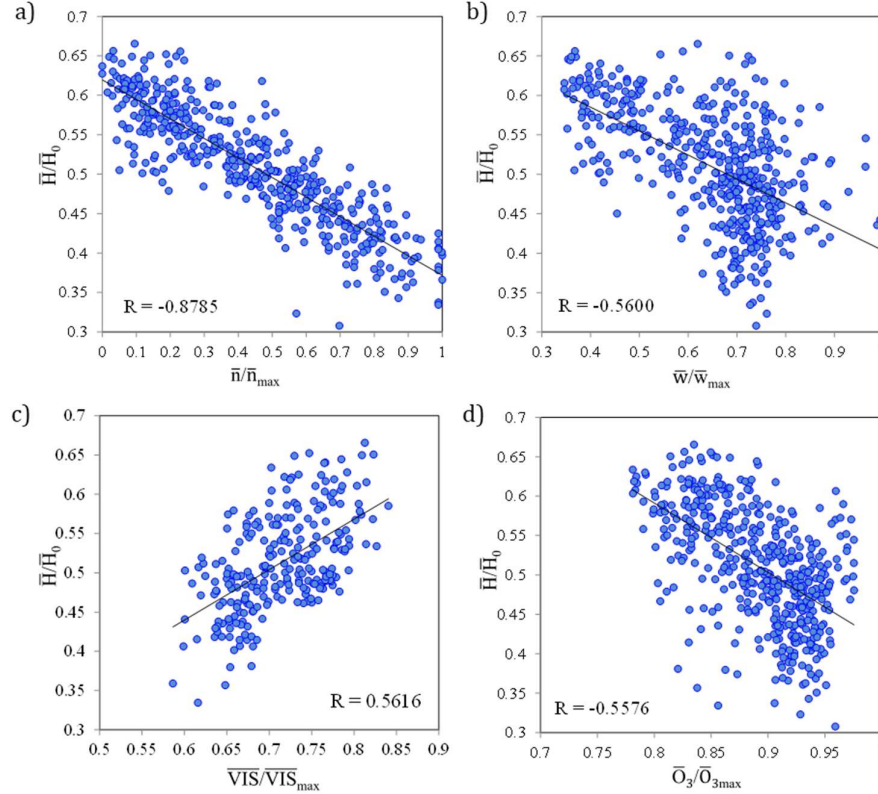


Figure 2. Dependence of normalized monthly average of daily global solar irradiation on the amount of various atmospheric constituents: a) normalized cloud index b) normalized precipitable water c) normalized visibility, and d) normalized total ozone column

From Figure 2, we also noticed that the normalized values of the cloud index, precipitable water, total ozone column, and visibility linearly affected the normalized value of the monthly average of daily solar irradiation.

Equation 3 was fitted with solar irradiation and the related data at the four solar monitoring stations, encompassing a 10-year period (2006-2015) to obtain the coefficients of the model. \bar{H}_0 was calculated using a formula given by Iqbal (1983). The coefficients and statistical parameters obtained from the statistical analysis are presented in Table 1.

To evaluate the model's performance, the model in computing the solar irradiation at 36 solar monitoring stations of DEDE was used (Figure 1). The results were compared with those obtained from the measurement (Figure 3 and Table 2).

The results from Figure 3 indicated that \bar{H}_{model} agreed well with \bar{H}_{measure} , with the discrepancy reflected in the root mean square difference (RMSD) relative to the mean measured irradiation of 6.9% and the mean bias difference

(MBD) relative to the mean measured irradiation of 1.0%. Janjai et al. (2013b) used a physical model to calculate solar radiation. They found that the solar radiation calculated from the model and that obtained from the measurement had an RMSD of 5.3% and MBD of 0.3%. Bosch et al. (2010) used Heliosat-2 together with a digital terrain model to calculate the solar radiation over an area in Spain and found that the solar radiation calculated from the model and that from the measurement were in agreement, with the RMSD being 10% and the MBD being 2%. Polo et al. (2011) employed a satellite approach to estimate the solar radiation over India and found that the solar radiation calculated from the satellite and that from measurements were in reasonable agreement, with the RMSD being around 12% and the MBD being around 5%. Polo (2015) used a satellite approach to derive solar irradiation over Spain and found that the comparison between satellite-derived global solar irradiation and that from the measurements had the RMSD of 11%. Therefore, the accuracy of the proposed model was comparable to that in published works.

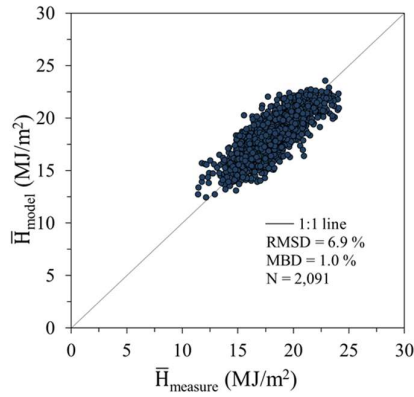


Figure 3. Comparison between monthly average of daily global solar irradiation calculated from the model (\bar{H}_{model}) and that obtained from the measurement (\bar{H}_{measure})

Table 2. Names, latitudes, longitudes, and altitudes of DEDE stations whose data were used to evaluate the model's performance

No.	Station	Latitude (degree)	Longitude (degree)	Altitude (m)	Period of data	RMSD (%)	MBD (%)
1	Chiang Rai	20.08	99.88	495	Oct 2012-Dec 2015	8.8	5.0
2	Mae Hong Son	19.43	97.96	730	Jan 2011-Dec 2015	11.7	7.2
3	Nan	18.72	100.75	459	Jan 2011-Dec 2015	7.3	3.9
4	Chiang Mai (Sansai)	18.83	98.88	565	Jan 2011-Dec 2015	7.9	3.5
5	Mae Sa Rieng	18.17	97.93	698	Jan 2011-Dec 2015	8.0	5.0
6	Phrae	18.06	100.06	390	Jan 2011-Dec 2015	5.4	-1.0
7	Tak	16.80	98.90	562	Jan 2011-Dec 2015	7.9	-0.3
8	Loei	17.40	101.00	492	Jan 2011-Dec 2015	6.1	2.0
9	Nong Khai	17.87	102.72	177	Jan 2011-Dec 2015	5.0	-2.1
10	Khon Kaen	16.45	102.78	179	Jan 2011-Dec 2015	6.2	-1.7
11	Nakhon Panom	16.97	104.73	184	Jan 2011-Dec 2015	7.3	0.0
12	Surin	14.88	103.50	162	Jan 2011-Dec 2015	7.4	0.2
13	Ubon Ratchathani (Agr. Met)	15.28	105.14	160	Jan 2011-Dec 2015	5.3	0.2
14	Nakhon Ratchasima	14.97	102.08	218	Jan 2011-Dec 2015	6.3	2.3
15	Roi Et	16.07	103.00	153	Jan 2011-Dec 2015	5.2	-0.7
16	Phitsanulok	16.78	100.27	137	Jan 2011-Dec 2015	6.2	3.1
17	Phetchabun	16.43	101.15	250	Jan 2011-Dec 2015	4.8	2.2
18	Nakhon Sawan	15.67	100.12	50	Jan 2011-Dec 2015	4.5	2.5
19	Lop Buri	14.83	100.62	54	Jan 2011-Dec 2015	6.7	1.1
20	Bangkok	13.75	100.52	2	Jan 2011-Dec 2015	8.5	4.9
21	Kanchanaburi (Muang)	14.02	99.53	159	Jan 2011-Dec 2015	5.1	-0.9
22	Kanchanaburi (Thong Pha Phum)	14.73	98.63	345	Jan 2011-Dec 2015	7.5	2.4
23	Sa Kaeo (Aranyaprathet)	13.70	102.00	62	Jan 2011-Dec 2015	5.5	2.7
24	Trat	11.77	102.88	68	Jan 2011-Dec 2015	8.8	-3.0
25	Prachin Buri	13.97	101.70	46	Jan 2011-Dec 2015	5.0	1.3
26	Chon Buri	13.37	100.97	5	Jan 2011-Dec 2015	6.7	0.5
27	Prachuap Khiri Khan	11.83	99.83	1	Jan 2011-Dec 2015	6.3	-3.3
28	Hua Hin	12.59	99.73	107	Jan 2011-Dec 2015	3.2	0.8
29	Chumphon	10.40	99.18	8	Jan 2011-Dec 2015	7.4	2.4
30	Ranong	9.98	98.62	34	Jan 2011-Dec 2015	7.4	-0.2
31	Surat Thani (Samui)	9.47	100.05	1	Jan 2011-Dec 2015	7.7	-4.6
32	Surat Thani (Punpin)	9.13	99.15	10	Jan 2011-Dec 2015	6.5	1.5
33	Phuket	8.13	98.30	26	Jan 2011-Dec 2015	6.2	-3.8
34	Trang	7.52	99.62	55	Jan 2011-Dec 2015	8.4	0.6
35	Songkhla (Hadyai)	6.92	100.43	53	Jan 2011-Dec 2015	6.9	3.5
36	Narathiwat	6.40	101.82	8	Jan 2011-Dec 2015	6.7	1.7
Combined data						6.9	1.0

Note: This table also shows the data period and the values of the root mean square difference (RMSD) relative to the mean measured irradiation and the mean bias difference (MBD) relative to the mean measured irradiation.

In mapping the monthly average of daily irradiation over Thailand, the values of all model parameters encompassing the whole areas of the country must be obtained. As precipitable water (w) was calculated from the temperature (T_a) and relative humidity (rh_a) of the air, the values of T_a and rh_a measured at the 80 meteorological stations were interpolated to obtain their values at the position corresponding to the pixels of the MTSAT-1R. In addition, the interpolated values of T_a and rh_a were employed to calculate w . A similar approach was used to estimate visibility. Finally, the values of w , VIS, O_3 , and n were used to calculate solar irradiation using the model (Equation 3). The outcomes were displayed as solar irradiation maps (Figures 4 and 5).

The monthly irradiation maps (Figure 4) showed that the solar irradiation at most of the locations around the country gradually increased in January, peaks in April, and

then gradually decreased toward the end of the year. In the yearly irradiation map (Figure 5), the areas with the highest irradiation were observed to be situated in the lower part of the northeastern region and some areas in the central region. Solar irradiation was relatively low in the mountain ranges in the north and in the western parts of Thailand. Low solar irradiation areas were found in the western part during the southwest monsoon period (May–September) and in the eastern part of the southern region during the northeast monsoon (October–January). This result was most likely due to the abundance of clouds in these areas during these periods (Charuchittipan et al., 2018). Overall, the patterns of the geographical distribution of solar irradiation obtained from this approach are similar to those obtained from the sophisticated physical model (Janjai et al., 2013a).

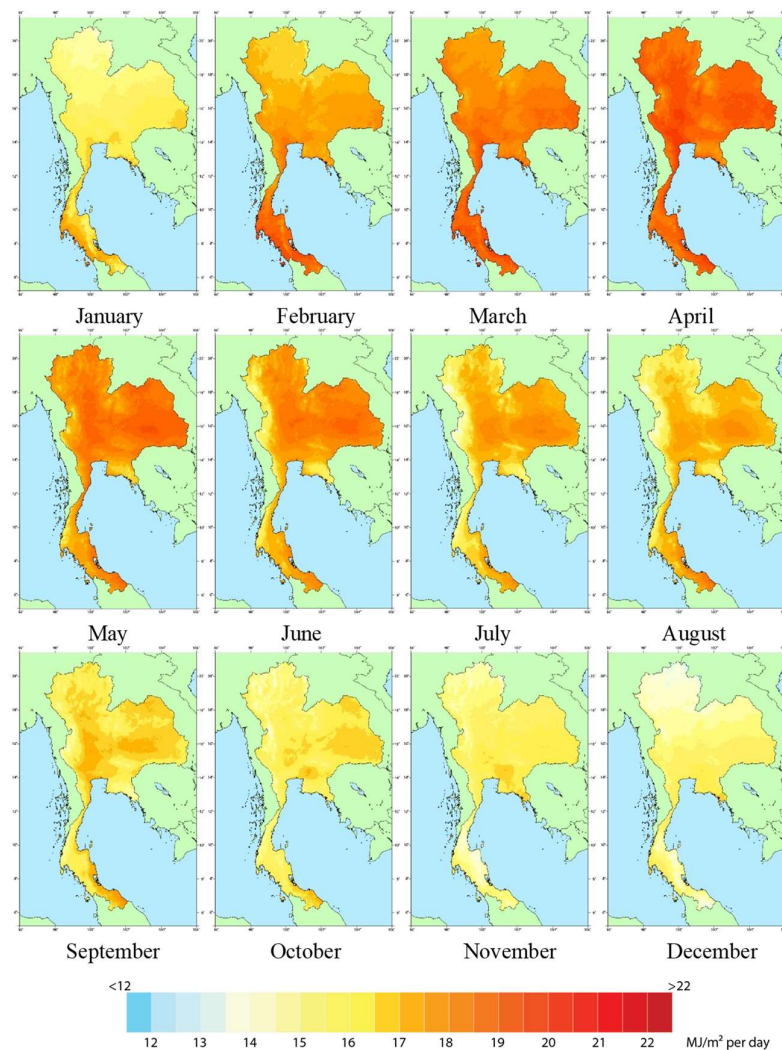


Figure 4. Monthly solar irradiation map of Thailand

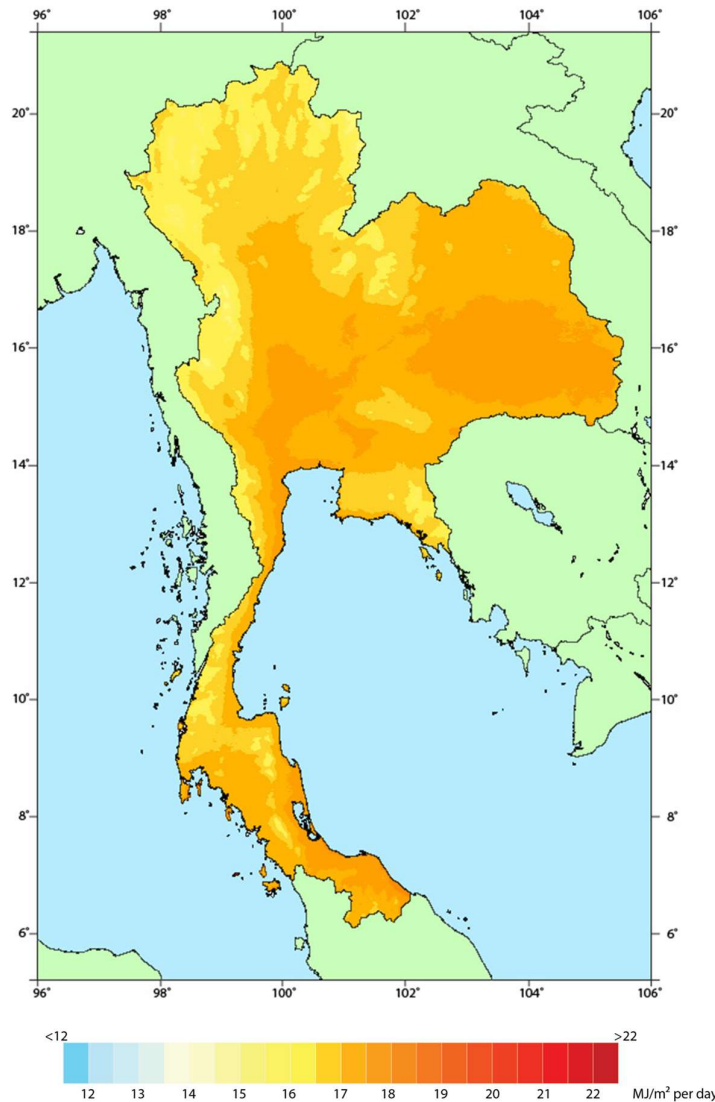


Figure 5. Yearly solar irradiation map of Thailand

4. CONCLUSION

An approach to mapping surface solar irradiation was developed using the calculation of solar irradiation from a simple semi-empirical model. The compositions of the atmosphere affecting the incoming solar irradiation were involved empirically in the model. The data on these compositions are commonly available, thus facilitating the modeling and mapping processes. The model performance is comparable to that of sophisticated models, but the proposed model is relatively simple. Our solar irradiation maps demonstrated the effects of the geographic features of terrains and those of monsoons. We concluded that the proposed method is feasible for mapping solar irradiation in Thailand.

ACKNOWLEDGMENT

Mr. Wanchalerm Chanalert, the first author received financial support from Thailand Science Research and

Innovation (TSRI, formerly named Thailand Research Fund (TRF)) through the Royal Golden Jubilee (RGJ) Ph. D. program (Grant number PHD/0201/2559). The first author would like to thank TSRI for this support. The authors would also like to thank the DEDE and the Thai Meteorological Department for providing the data needed for this study.

REFERENCES

- Bosch, J. L., Batlles, F. J., Zarzalejo, L. F., and López, G. (2010). Solar resources estimation combining digital terrain models and satellite images techniques. *Renewable Energy*, 35(12), 2853-2861.
- Cano, D., Monget, J. M., Albuissou, M., Guillard, H., Regas, N., and Wald, L. (1986). A method for the determination of the global solar radiation from meteorological satellite data. *Solar Energy*, 37(1), 31-39.
- Charuchittipan, D., Janjai, S., Pratummasoot, N., Buntoung, S., and Peengam, S. (2018). Mapping of cloud cover

- from satellite data over Thailand. *Science, Engineering and Health Studies*, 12(2), 69-76.
- Department of Alternative Energy Development and Efficiency. (2007). *Assessment of Solar Energy Potentials for Lao People's Democratic Republic*. Bangkok: Department of Alternative Energy Development and Efficiency, pp. 48-50.
- Department of Alternative Energy Development and Efficiency. (2009). *Assessment of Solar Energy Potentials for Myanmar*. Bangkok: Department of Alternative Energy Development and Efficiency, pp. 71-72.
- Dhaka, C. P. (2019). Interpreting the basic outputs (SPSS) of multiple linear regression. *International Journal of Science and Research*, 8(6), 1448-1452.
- Duffie, J. A., and Beckmann, W. A. (2013). *Solar Engineering of Thermal Process*, 4th, New Jersey: John Wiley & Sons Inc., pp. 138-173.
- Exell, R. H. B. (2007). Mapping solar radiation by meteorological satellite. *Renewable Energy Review Journal*, 6(1), 27-39.
- Huang, G., Li, Z., Li, X., Liang, S., Yang, K., Wang, D., and Zhang, Y. (2019). Estimating surface solar irradiance from satellites: past, present, and future perspectives. *Remote Sensing of Environment*, 233, 111371.
- Iqbal, M. (1983). *An Introduction to Solar Radiation*, Cambridge, MA: Academic Press, pp. 128-133.
- Janjai, S., Laksanaboonsong, J., Nunez, M., and Thongsathitya, A. (2005). Development of a method for generating operational solar radiation maps from satellite data for a tropical environment. *Solar Energy*, 78(6), 739-751.
- Janjai, S., Masiri, I., and Laksanaboonsong, J. (2013a). Satellite-derived solar resource maps for Myanmar. *Renewable Energy*, 53, 132-140.
- Janjai, S., Masiri, I., Pattarapanitchai, S., and Laksanaboonsong, J. (2013b). Mapping global solar radiation from long-term satellite data in the tropics using an improved model. *International Journal of Photoenergy*, 2013, 210159.
- Kämpfer, N. (2013). Introduction. In *Monitoring Atmospheric Water Vapour: Ground-Based Remote Sensing and In-situ Methods (ISSI Scientific Report Series, 10)* (Kämpfer, N., ed.), pp. 1-7. New York, NY: Springer.
- Montgomery, D. C., Peck, E. A., and Vining, G. G. (2012). *Introduction to Linear Regression Analysis*, 5th, New Jersey: John Wiley & Sons, Inc., pp. 12-58.
- Möser, W., and Raschke, E. (1984). Incident solar radiation over Europe estimated from METEOSAT data. *Journal of Climate and Applied Meteorology*, 23(1), 166-170.
- Pinker, R. T., and Laszlo, I. (1992). Modeling surface solar irradiance for satellite applications on a global scale. *Journal of Applied Meteorology and Climatology*, 31(2), 194-211.
- Polo, J., Zarzalejo, L. F., Cony, M., Navarro, A. A., Marchante, R., Martin, L., and Romero, M. (2011). Solar radiation estimations over India using Meteosat satellite images. *Solar Energy*, 85(9), 2395-2406.
- Polo, J. (2015). Solar global horizontal and direct normal irradiation maps in Spain derived from geostationary satellites. *Journal of Atmospheric and Solar-Terrestrial Physics*, 130-131, 81-88.
- Press, W. H., Teukolsky, S. A., Vetterling, W. T., and Flannery, B. P. (1992). *Numerical Recipes in Fortran 77*, 2nd, Cambridge: Cambridge University Press, p. 994.
- Salby, M. L. (1996). *Fundamentals of Atmospheric Physics*. New York: Academic Press, pp. 1-648.
- Sorapipatana, C., Exell, R. H., and Borel, D. (1988). A bispectral method for determining global solar radiation from meteorological satellite data. *Solar & Wind Technology*, 5(3), 321-327.
- Suwantragul, B., Watrabutr, W., Sitathani, K., Tia, V., and Namprakai, P. (1984). *Solar and Wind Energy Potential Assessment of Thailand*, Bangkok: King Mongkut's Institute of Technology Thonburi Campus, pp. 423-433.
- Wyser, K., O'Hirok, W., Gautier, C., and Jones, C. (2002). Remote sensing of surface solar irradiance with corrections for 3-D cloud effects. *Remote Sensing of Environment*, 80(2), 272-284.